THE ROLE OF PHASE CHANGES DURING IMPACT CRATERING ON ICY SATELLITES. L. E. Senft and S. T. Stewart. Department of Earth & Planetary Sciences, Harvard University, 20 Oxford St., Cambridge, MA 02138, U.S.A. (lsenft@fas.harvard.edu)

Introduction: Models of impact cratering on the icy satellites have been used to suggest the presence of transient liquid water [1-4] and to infer the thickness of brittle crusts [5]. These studies rely strongly on the accuracy of the equation of state (EOS) of H_2O to determine the peak and post shock pressures and temperatures. In the past, EOS models for H_2O (such as ANEOS [5], Mie-Grüneisen, and Tillotson – see Appendix II in [6]) have typically been simplified, ignoring conversions to high-pressure solid phases and inaccurately representing the melting and vapor curves. Here we use a new tabular EOS for H_2O, the 5-Phase EOS [7, 8], to model impact cratering on the icy satellites. This EOS includes high-pressure ice phases, liquid, and vapor.

We find that including the high-pressure solid phases produces more complex crater formation phenomenology, including changes in the excavation flow that lead to a concentration of highly shocked material in the crater floor. High-pressure ice phase transformations may help to explain the wide range of crater morphologies observed on the icy planets and satellites [e.g. 9].

Method: To illustrate a subset of icy cratering phenomena, we conducted simulations of impacts onto the Jovian satellite Ganymede using our modified version of the shock physics code CTH [10, 7] . Ice impactor diameters ranged from 100 m to 5 km, and the impact velocity was 15 km/s. The surface temperature was assumed to be 120 K. Warm and cold geotherms were considered, representing conditions in the early solar system and present day, respectively. We utilize the quasi-static strength model for ice derived in [11]. To achieve the appropriate amount of crater collapse, we used the acoustic fluidization model [12] with acoustic fluidization parameters as determined for the moon [13]. A recent study has shown that the lunar acoustic fluidization parameters (surface gravity of 1.62 m/s^2) are appropriate for use on Ganymede (surface gravity of 1.43 m/s^2) [14]. Final crater diameters ranged between about 10 and 90 km.

The new 5-Phase EOS is a tabular EOS. Thus, there are no limitations on the number of phases that may be included, but phase boundaries need to be carefully gridded. The 5-Phase EOS includes three solid phases (ices Ih, VI, and VII), liquid and vapor. The EOS of the phases and phase boundaries are experimentally determined. The liquid and vapor are described by the International Association for the Properties of Water and Steam (IAPWS) [15]. The EOS of ice Ih is given by [16]. The EOS of ices VI and VII are taken from [17], and the phase boundaries are given by [15, 18]. The phase boundary between ice Ih and VI is artificial: ice phases II, III, and V are neglected and the ice VI field is extended in pressure-temperature space to meet ice 1h.

Results:

Changes in crater phenomenology: Inclusion of high-pressure ice phases in the EOS changes the excavation flow process and forms a detached layer of highly shocked material (Figure 1). During propagation of the impact-generated shock wave, ice Ih is shocked to vapor, liquid, high-pressure ice phases (VII and VI), and then ice Ih with increasing distance from the impact point (Figure 1A). Hence, the release wave travels through layers of different phases of H_2O. The different release paths between adjacent layers with different impedances changes the excavation flow compared to a homogeneous (or more impedance matched) material.

Because transformation from the high-pressure solid ice phases back to ice Ih requires a large volume increase (e.g., ~30% from ice VI to ice Ih), full release of the high-pressure ice phases is delayed until the volume change can be accommodated in the excavation flow. The back transformation to ice Ih occurs progressively from the free surface to greater depths. As the high-pressure phases fully release, a vapor-rich layer is formed and the hotter material is separated from the crater walls (Figure 1B). The hot material initially releases to the saturation vapor curve; the material must cool by vaporizing in order to fully decompress [see 8].

The different excavation flow concentrates the hot material in the center of the crater floor rather than lining the entire cavity (or being ejected). During crater collapse, the pool of hot material in the crater center may be fully or partially buried (Figure 1C). The end result is a central hot plug of material that is either fully or partially liquid. The amount and final configuration of the hot plug is sensitive to the size of the crater, the geotherm, the crater collapse mechanism, and the kinetics of the back transformations (which requires experimental investigation). The fate of the hot plug depends on

the exact geometry and surrounding temperature-pressure conditions. In some cases, gravitationally-driven rebound aids decompression and conversion to vapor phases by causing pressure fluctuations. It is possible that this vapor may be released in explosive events, forming morphologies similar to central pits [e.g. 19].

Comparisons to other EOS models: We compared shock pressure decay profiles for the 5-Phase EOS with pressure decay profiles for ANEOS [5] in a 120 K isothermal ice target. We found that ANEOS tends to overestimate the peak shock pressure, underestimate the pressure decay with distance, and underestimate the peak shock temperature. As a result, volumes of melt calculated from ANEOS using a peak pressure criteria of ~2 GPa tend to overestimate the volumes by a factor of about 1.5 to 2.0. The Tillotson EOS also neglects high pressure phase changes. In addition, melting is ignored and vaporization on release is not accurately modeled. The Mie-Grüneisen EOS only represents one phase (although simple compound phase models may be assembled). Thus, neither Tillotson, Mie-Grüneisen, or ANEOS can capture the phenomenology studied here. Finally, the post-shock temperatures calculated by all three of these models are generally inaccurate. In the future, a new version of ANEOS [20] may provide a better model for H_2O; however it is still limited in the number of phases (e.g., either liquid or a high pressure solid phase). We note that in some limited problems, these simplified EOSs may be adequate approximations; however, any problem that relies upon real temperatures (for example strength modeling) or accurate phase changes on release will require a more detailed EOS.

Conclusions: Including high-pressure ice phases in cratering calculations modifies crater excavation and leads to interesting phenomena. More accurate equations of state of H_2O lead to better estimates of melt and vapor volumes and allow the state and location of water and vapor to be better tracked during the crater formation process. Thus, the 5-Phase EOS will be useful in interpreting the variety of crater morphologies seen on the icy satellites as well as constraining the thickness of brittle crusts.

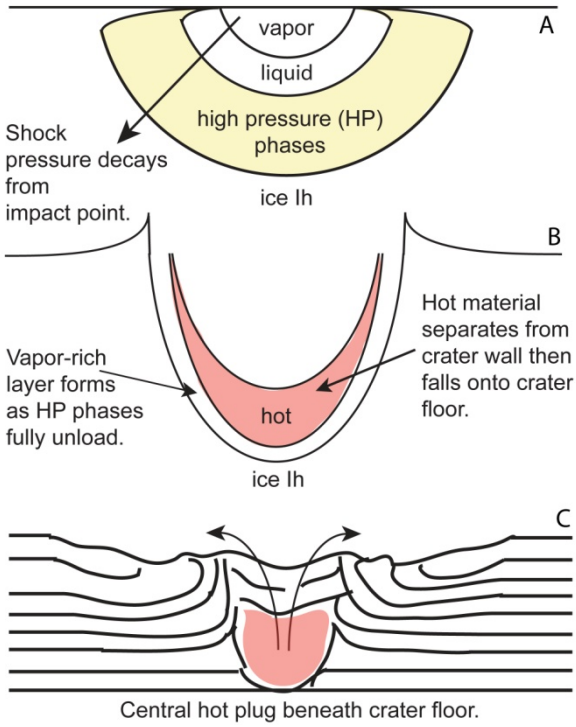

Figure 1: Schematic of an impact cratering event on an icy satellite.

References: [1] Artemieva, N. and J.I. Lunine (2005) *Icarus* **175**, 522. [2] Artemieva, N. and J. Lunine (2003) *Icarus* **164**, 47. [3] Pierazzo, E., N.A. Artemieva, and B.A. Ivanov (2005) **GSA** *384*, 443. [4] Stewart, S.T., J.D. O'Keefe, and T.J. Ahrens (2004) *Shock Comp. Cond. Mat. – 2003*, 1484. [5] Turtle, E.P. and E. Pierazzo (2001) *Science* **394**, 1326. [6] Melosh, H.J. *Impact Cratering*, Oxford U. Press (1999). [7] Senft, L.S. and S.T. Stewart (2009) *MAPS*, in press. [8] Stewart, S.T., A. Seifter, and A.W. Obst (2008) *GRL* **35**, doi: 10.1029/2008GL035947. [9] Schenk, P.M. (2002) *Nature* **417**, 419. [10] Senft, L.S. and S.T. Sewart (2007) *JGR* **112**, doi: 10.1029/2007JE002894. [11] Collins, G.S., H. J. Melosh, and B.A. Ivanov (2004) *MAPS* **39**, 217. [12] Melosh, H.J. and B.A. Ivanov (1999) *Ann. Rev. Earth Planet. Sci.* **27**, 385. [13] Wunnemann, K. and B.A. Ivanov (2003) *Planet. Space Sci.* **51**, 831. [14] Bray, V.J., G.S. Collins, J.V. Morgan, and P.M. Schenk (2009) *MAPS*, in press. [15] Wagner, W. and A. Pruss (2002) *JPCRA* **31**, 387. [16] Feistel, R. and W. Wagner (2006) *JPCRA* **35**, 1021. [17] Stewart, S.T. and T.J. Ahrens (2005) *JGR* **110**, E03005. [18] Frank, M.R., Y.W. Fei, and J.Z. Hu (2004) *Geo. Cos. Acta* **68**, 2781. [19] Schenk, P. M. (1993) *JGR* **98**, 7475. [20] Melosh, H.J. *MAPS* **42**, 2079.